Available online at http://www.advancedscientificjournal.com
http://www.krishmapublication.com
IJMASRI, Vol. 2, issue 3, pp. 452-463, March -2022
https://doi.org/10.53633/ijmasri.2022.2.3.004

INTERNATIONAL JOURNAL OF MULTIDISCIPLINARY ADVANCED SCIENTIFIC RESEARCH AND INNOVATION (IJMASRI)

ISSN: 2582-9130 IBI IMPACT FACTOR 1.5 DOI: 10.53633/IJMASRI

RESEARCH ARTICLE

EFFECT ON VISCOUS DISSIPATION, FREE CONVECTION RADIATION AND MASS TRANSFER OF THREE DIMENSIONAL CASSON FLUID EMBEDDED IN AN INCLINED STRETCHING SHEET WITH HALL CURRENT

[1]Valsamy P, [2]Sheela D and [3]Nirmala P. Ratchagar

[1]Engineering Mathematics, FEAT Annamalai University, Annamalainagar, Chidambaram – 608 002, Tamilnadu, India.
[2,3] Department of Mathematics, Annamalai University, Annamalainagar,Chidambaram– 608002, Tamilnadu, India
E-mail: valsamy@yahoo.co.in , sheelasastra15@gmail.com , nirmalapasala@yahoo.co.in

Abstract

This paper aims to described unsteady free convection flow with Casson fluid through an inclined permeable stretched surface. In the presence of viscous dissipation, heat generation or absorption, transfer of thermal radiation and mass are studied., The governing equations are transformed to the non-linear differential equation using the similarity approaches. Perturbation approach is applied to solve the resulting equations. Outcomes of the velocity field, temperature profile and concentration field are discussed through graphs.

Key words: Inclined stretching sheet, Casson fluid, Hall current, Radiation, Viscous dissipation.

Introduction

Pioneering the fluid flow of non-Newtonian model through a stretching sheet has wide range of industrial applications. Example of non-Newtonian fluids is slurries, quick sand, biological fluids, polymer solutions and paints.

Mukhopadhyay *et.al.,* (2013) investigated numerical result of prescribed surface temperature and Casson fluid through a stretched surface. (Nadeem *et.al.*, 2013) discussed Casson fluid embedded in a MHD permeable surface of linear stretched area. (Manhanta and Shaw, 2015) analyzed boundary layer three-dimensional MHD electrical conducting Casson fluid towards a linear permeable stretching medium with convective condition and heat radiation. (Raju *et.al.*, 2016) scrutinized the outcome of radiation, viscous dissipation, magnified heat source with chemical rate reaction past an exponentially stretched medium of MHD Casson fluid and also compared the results with Newtonian fluid. Imran (ullah *et.al.*, 2014) reviewed Casson fluid along MHD saturated stretching of nonlinear channel with slip condition, free convection and Newtonian heating.

(Eswara Rao, 2017) examined numerical study of Casson fluid towards an inclined exponential stretching medium with Brownian motion, thermophoresis effect, heat radiation and chemical rate reaction. Assessed MHD boundary layer entropy generation along a impermeable inclined stretched channel in the occurence of mixed convection, viscous heating and non-isothermal condition. Srinivasa raju *et.al.*, (2017) examined magnetohydrodynamic optically thick Casson fluid through the inclined vertical surface including natural convection, radiation and mass transfer by applying finite element procedure. (Manjula and Chandra Sekhar, 2020) investigated natural convective flow of Casson fluid over a permeable inclined surface existing of viscous dissipation, heat radiation and magnetic induction. (Pavan kumar *et.al.*, 2021) discussed electrical conducting Casson fluid towards an oscillating inclined porous medium with free convection, Soret effect, thermal diffusion, heat absorption, radiation and mass transfer.(Tabaei et.al., 2011] exhibited magnetohydrodynamic free convective electrically conducting viscous fluid flow embedded in stretched sheet by the outcome of Hall effect and chemical rate reaction by applying homotopy method. Interpreted the analysis of MHD steady state electrically fluid flow through an inclined stretched sheet under the impact of Hall effect, heat radiation and mass transport. (Ali and Alam, 2014) discussed the numerical approach of MHD two dimensional electrically conducting flow with Hall effect, generation of heat, Soret and Dufour effects towards the vertical permeable stretching sheet. (Bilal Ashraf *et.al.*, 2017) scrutinized flow of Casson model on a stretched surface in the impact of Hall effect, mixed convection, heat radiation and mass transfer. (Shateyi *et.al.*, 2017) exhibited free convective Casson fluid along a stretched permeable channel considering the magnetic field, viscous dissipation, radiation and mass transfer utilized by Runge Kutta Fehlberg method.

The outcome of Hall current, free convection flow, thermal radiation, viscous dissipation, heat generation/absorption and chemical reaction through an inclined stretching surface with the angle of inclination α is studied in this paper. Perturbation method is used to study the flow model. The graphs are presented for velocity, thermal profile and concentration distribution by using Mathematica software.

Mathematical formulation

We consider an unsteady three dimensional Casson fluid flow past a stretching inclined surface in the presence of Hall effects, free convection, thermal radiation, viscous dissipation, heat generation or absorption and rate of chemical reaction. It is assumed that x-axis parallel to the sheet surface and z-axis taken transverse of the *xy*-plane. The magnetic induction $B(t)$ is applied vertical direction to the flow field. The presence of Hall effect creates a three dimensional flow by generating a force along z-axis which creates a counterflow in that path. $U_w(x) = \frac{ax}{1-bt}$ is the flow rate of stretched sheet. Sheet temperature and concentration is defined by T_w and C_w following from $T_w = T_\infty + \theta(\frac{cx}{(1-bt)^2})$, $C_w = C_\infty + \varphi(\frac{cx}{(1-bt)^2})$, where c is constant with c=0 for forced convection.

The modified generalized Ohm's law, which takes into account Hall current described by

$$\boldsymbol{J} + (\omega\_e\ \tau\_e)/\boldsymbol{B}\ (\boldsymbol{J} \times \boldsymbol{B}) = \sigma(\boldsymbol{E} + V \times \boldsymbol{B}) \qquad (1)$$

Where $\boldsymbol{J} = (j_x, j_y, j_z)$, $\boldsymbol{B} = (0, B_0, 0)$, $V = (u, 0, w)$, $\boldsymbol{E} = (E_x, E_y, E_z)$, ω_e, τ_e and σ define components of current density vector, vector component of magnetic field, velocity components, vector component of magnetic field, velocity components, vector component of electric field, cyclotron frequency, electron collision time and electric conductivity. Hall current are stimulated in the existence of large magnetic field. The Lorentz force $J \times B$ induces the Hall effect. The flow will turns two dimension when Hall current cause when secondary flow. J_y =Constant is the outcome of the conservation of electric $\nabla \cdot J = 0$. $J_y = 0$ everywhere in the flow because the magnetic sheet's surface is electrically insulating. Furthermore, when there is no voltage applied. The electric field vanishes, resulting in E=0. The current primary and secondary current density components are used. From the above equation we get

$$j_x = \frac{\sigma \mu_e H_0}{1+m^2}(mu - w) \quad (2)$$

$$j_z = \frac{\sigma \mu_e H_0}{1+m^2}(u + mw) \quad (3)$$

For an incompressible Casson fluid, the isotropic rheological equation is denoted as, (Mustafa, *et.al.*, 2011)

$$\tau_{ij} = \begin{cases} \left(\frac{\mu_B + P_y}{\sqrt{2\pi}}\right) 2e_{ij}, & \pi > \pi_c \\ \left(\frac{\mu_B + P_y}{\sqrt{2\pi_c}}\right) 2e_{ij}, & \pi < \pi_c \end{cases} \quad (4)$$

where μ_B, P_y, $\pi = e_{ij}e_{ij}$ and π_c are defined the plastic dynamic viscosity, yield stress, rate of product deformation of $(i, j)th$ component, critical value.

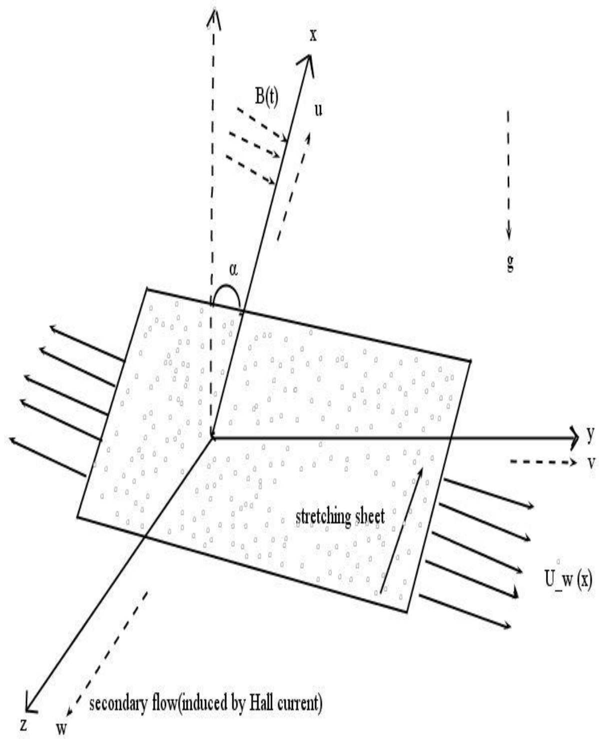

Fig. 1: Physical configuration of the model.

Governing equations of the present model are

$$\frac{\partial u}{\partial x} + \frac{\partial v}{\partial y} + \frac{\partial w}{\partial z} = 0 \quad (5)$$

$$\frac{\partial u}{\partial t} + u\frac{\partial u}{\partial x} + v\frac{\partial u}{\partial y} + w\frac{\partial u}{\partial z} = \nu\left(1 + \frac{1}{\beta}\right)\frac{\partial^2 u}{\partial y^2} + g\beta_T(T - T_\infty)cos\alpha + g\beta_T(C - C_\infty)cos\alpha$$
$$+ \frac{\nu}{k'}u + \frac{\sigma B^2(t)}{\rho(1+m^2)}(u + mw) \quad (6)$$

$$\frac{\partial w}{\partial t}+u\frac{\partial w}{\partial x}+v\frac{\partial w}{\partial y}+w\frac{\partial w}{\partial z}=\left(1+\frac{1}{\beta}\right)\frac{\partial^2 w}{\partial y^2}+\frac{\sigma B^2(t)}{\rho(1+m^2)}(mu-w) \quad (7)$$

$$\frac{\partial T}{\partial t}+u\frac{\partial T}{\partial x}+v\frac{\partial T}{\partial y}+w\frac{\partial T}{\partial z}=\frac{\kappa}{\rho c_p}\frac{\partial^2 T}{\partial y^2}-\frac{1}{\rho c_p}\frac{\partial q_r}{\partial y}+\frac{\mu}{c_p}\left(1+\frac{1}{\beta}\right)\left(\frac{\partial u}{\partial y}\right)^2+\frac{Q}{\rho c_p}(T-T_\infty) \quad (8)$$

$$\frac{\partial C}{\partial t}+u\frac{\partial C}{\partial x}+v\frac{\partial C}{\partial y}+w\frac{\partial C}{\partial z}=D\frac{\partial^2 C}{\partial y^2}+K_0(C-C_\infty) \quad (9)$$

here u, v and w indicates velocity over the direction x, y and z. t refers time, v kinematic viscosity, β denotes Casson fluid parameter, g defines acceleration gravity, α indicates angle of inclination, k' denotes permeability, σ describes electrical conductivity, m *defines* Hall current term, T represents temperature, κ denotes thermal conductivity, c_p is specific heat, q_r denotes heat flux, μ fluid viscosity, C concentration, D diffusivity, K_0 chemical reaction parameter Variable magnectic field is denoted by $B(t)=\frac{B}{\sqrt{1-\gamma t}}$, where β and γ are constants.

The corresponding boundary conditions are represented by,

$$\left.\begin{array}{l} u=U_w, v=w=0, T=T_w, C=C_w \quad at\ y=0 \\ u\to 0, w\to 0, T\to T_\infty, T\to T_\infty\ at\ y=\infty \end{array}\right\} \quad (10)$$

q_r denotes approximated Rosseland raditive heat flux is represented as (Turkyilmazoglu, 2011)

$$q_r=-\frac{4\sigma^*}{3k^*}\frac{\partial T^4}{\partial y} \quad (11)$$

here σ^* and k^* indicates constant of Stefan's and absorption of mean coefficient. Extending the T^4 in expansion of Taylor series over T_∞ and omitting the higher terms we get,

$$T^4\approx 4T_\infty{}^3T-3T_\infty{}^4 \quad (12)$$

substituting the eqn(12) in eqn(11) we get,

$$q_r=-\frac{4\sigma^*\partial(4T_\infty{}^3T-3T_\infty{}^4)}{3k^*\partial y^*}$$

$$q_r=-\frac{16T_\infty{}^3}{3k^*}\frac{\partial T}{\partial y} \quad (13)$$

applying equation(13) in equation(8) we get,

$$\frac{\partial T}{\partial t}+u\frac{\partial T}{\partial x}+v\frac{\partial T}{\partial y}+w\frac{\partial T}{\partial z}=\frac{k}{\rho c_p}\left(1+\frac{16\sigma^*T_\infty{}^3}{3kk^*}\right)\frac{\partial^2 T}{\partial y^2}+\frac{\mu}{c_p}\left(1+\frac{1}{\beta}\right)\left(\frac{\partial u}{\partial y}\right)^2+\frac{Q}{\rho c_p}(T-T_\infty) \quad (14)$$

The following non-dimensional similarity transformation are introduced by,

$$\left.\begin{array}{l} u=\frac{ax}{1-bt}f'(\eta),\ v=-\sqrt{\frac{av}{1-bt}}f(\eta),\ w=\frac{ax}{1-bt}h(\eta), \\ \eta=\frac{a}{v(1-bt)}y,\ \theta(\eta)=\frac{T-T_\infty}{T_w-T_\infty},\ \varphi(\eta)=\frac{C-C_\infty}{C_w-C_\infty} \end{array}\right\} \quad (15)$$

where, the similarity parameter η and $f(\eta)$, $\theta(\eta)$ are the dimensionless variables. Now substituting Eq.(15) in Eqs.(6), (7), (14) and Eq.(9), the governing equations become

$$\left(1+\frac{1}{\beta}\right)f''' + A\frac{\eta}{2}f'' + ff'' - f'^2 - (A+K) + Gr\theta\cos\alpha$$

$$+Gc\varphi\cos\alpha + \frac{M}{(1+m^2)}(f'+mh) = 0 \tag{16}$$

$$\left(1+\frac{1}{\beta}\right)h'' + A\frac{\eta}{2}h' - f'h + fh' - Ah + \frac{M}{(1+m^2)}(mf-h) = 0 \tag{17}$$

$$(1+R)\theta'' + \Pr\left(A\frac{\eta}{2} - f\right)\theta' + \mathrm{Ec}\left(1+\frac{1}{\beta}\right)f'^2 + \lambda\theta = 0 \tag{18}$$

$$\varphi'' + Sc\left(A\frac{\eta}{2}\varphi' - f\varphi + \gamma\varphi\right) = 0 \tag{19}$$

the modified boundary conditions are:

$$\left.\begin{array}{c} f'(\eta) = 1, f(\eta) = h(\eta) = 0, \theta(\eta) = 1, \varphi(\eta) = 1 \; at \; \eta = 0 \\ f'(\eta) = 0, h(\eta) = 0, \theta(\eta) \to 0, \varphi(\eta) = 0 \; at \; \eta = \infty \end{array}\right\} \tag{20}$$

where *A, M, m, K, Gr, Gc, R, Pr, Ec, λ, Sc and γ* are defined as unsteadiness parameter, magnetic field parameter, Hall effect term, porosity parameter, Grashof number, locally modified Grashof number, radiation parameter, Prandtl number, Eckert number, heat generation/absorption term, Schmidth number and chemical reaction term.

The above dimensionless parameter denoted as

$$A=\frac{b}{a},\ M=\frac{\sigma B_0}{\rho a}, K=\frac{\nu(1-bt)}{k'a}, Gr=\frac{g\beta_T(T_w-T_\infty)}{a^2x}(1-bt)^2,\ Gc=\frac{g\beta_C(C_w-C_\infty)}{a^2x}(1-bt)^2,$$

$$R=\frac{16\sigma^* {T_\infty}^3}{kk^*},\ Pr=\frac{\mu c_p}{k},\ Ec=\frac{\nu(T_w-T_\infty)}{k}, \lambda=\frac{Q\nu(1-bt)}{ka},\ \mathrm{Sc}=\frac{\nu}{\mathrm{D}},\ \gamma=\frac{K_0(1-\mathrm{bt})}{a}.$$

Method of solution

The modified flow equations are resolved by Perturbation technique

$$\left.\begin{array}{c} f(\eta) = f_0(\eta) + \epsilon f_1(\eta) + \epsilon^2 f_2(\eta) + \cdots \\ h(\eta) = h_0(\eta) + \epsilon h_1(\eta) + \epsilon^2 h_2(\eta) + \cdots \\ \theta(\eta) = \theta_0(\eta) + \epsilon\theta_1(\eta) + \epsilon^2\theta_2(\eta) + \cdots \\ \varphi(\eta) = \varphi_0(\eta) + \epsilon\varphi_1(\eta) + \epsilon^2\varphi_2(\eta) + \cdots \end{array}\right\} \tag{21}$$

substituting the the eqn.(21) into eqns.(16) to (19), omitting the higher orderterms. we get,

Base part:

$$\left(1+\frac{1}{\beta}\right)f_0{}''' + A\frac{\eta}{2}f_0{}'' + f_0f_0'' - f_0{}'^2 - (A+K)f_0{}' + Gr\theta_0 cos\alpha$$

$$+Gc\varphi_0\cos\alpha + \frac{M}{(1+m^2)}(f_0{}' + mh_0) = 0 \qquad (22)$$

$$\left(1+\frac{1}{\beta}\right)h_0{}'' + A\frac{\eta}{2}h_0{}' - f_0{}'h_0 + f_0h_0{}' + Ah_0 + \frac{\mathrm{M}}{1+\mathrm{m}^2}(\mathrm{m}f_0 + h_0) = 0 \quad (23)$$

$$(1+R)\theta_0'' - Pr\frac{\eta}{2}A\theta_0' + Prf_0\theta_0' + \mathrm{Ec}\left(1+\frac{1}{\beta}\right)f_0{}''^2 + \lambda\theta_0 = 0 \qquad (24)$$

$$\varphi_0'' + \mathrm{Sc}\left(A\frac{\eta}{2}\varphi_0' + f_0\varphi_0' - \gamma\varphi_0\right) = 0 \qquad (25)$$

Perturbed part:

$$(1+\frac{1}{\beta})f_1{}''' + A\frac{\eta}{2}f_0'' + f_0f_1'' + f_1f_0'' - 2f_0'^{f_1} - (A+K)f_1{}' + Gr\theta_1 cos\alpha + Gc\varphi_1 cos\alpha +$$

$$\frac{\mathrm{M}}{1+\mathrm{m}^2}(\mathrm{m}f_1 + h_1) = 0 \qquad (26)$$

$$\left(1+\frac{1}{\beta}\right)h_1{}'' + A\frac{\eta}{2}h_1{}' - f_0{}'h_1 + f_0h_1{}' - Ah_1 + \frac{\mathrm{M}}{1+\mathrm{m}^2}(\mathrm{m}f_1 + h_1) = 0 \quad (27)$$

$$(1+R)\theta_1'' - Pr\frac{\eta}{2}A\theta_1' + Prf_0\theta_1' + Prf_1\theta_0' + Ec\left(1+\frac{1}{\beta}\right)f_0''\,f_1'' + \lambda\theta_1 \qquad (28)$$

$$\varphi_1'' + \mathrm{Sc}\left(A\frac{\eta}{2}\varphi_1' + f_0\varphi_1' + f_1\varphi_1' - \gamma\varphi_1\right) \qquad (29)$$

Base part boundary condition:

$$\left.\begin{array}{c} f_0{}^1 = 1, f_0 = 0, h_0 = 0, \theta_0 = 1, \varphi_0 = 1 \; at\; \eta = 0 \\ f_0{}^1 = 0, h_0 = 0, \theta_0 = 0, \varphi_0 = 0 \; at \; \eta = \infty \end{array}\right\} \qquad (30)$$

Perturbed part boundary condition:

$$\left.\begin{array}{c} f_1{}^1 = 1, f_1 = 0, h_1 = 0, \theta_1 = 1, \varphi_1 = 1 \; at\; \eta = 0 \\ f_1{}^1 = 0, h_1 = 0, \theta_1 = 0, \varphi_1 = 0 \; at \; \eta = \infty \end{array}\right\} \qquad (31)$$

The above base and perturbed part equations are solved subject to the boundary condition (30) and (31). Graphs are drawn for velocity distribution, temperature profile and concentration distribution employing by Mathematica software.

Result and discussion

The outcome of Casson fluid parameter, unsteadiness parameter, porous parameter, Grashof number, locally modified Grashof number, magnetic parameter, Hall current parameter over velocity field $f(\eta)$ are analyzed in the figures 2-8. The outcome of Casson fluid parameter is displayed in figure 2 which describes velocity field increase with increments of β. The impact of raising cases of unsteady parameter A is to increases the velocity field in figure 3. Velocity distribution $f\ (\eta)$ increases for various cases of porosity parameter which represented in the figure 4. The increasing cases of Grashof number leads increases the velocity field which displayed in figure 5. The raising values of locally modified Grashof number on velocity profile increases which shows in figure 6. The result of increment values of magnetic parameter and Hall current term over velocity raised in figure 7 and 8.

The outcome of Casson fluid, unsteady parameter, magnetic parameter, Hall current term over velocity profile $h(\eta)$ are demonstrated in the figure 9-12. The figure 9 demonstrates the result of β on velocity profile $h(\eta)$ which is parabolic in nature with raising values of β. The figure 10 exhibits the outcome of A on $h(\eta)$ which increasing and decreasing with raising values of A. The figure 11 represents the result of magnetic parameter over velocity that indicates $h(\eta)$ increases and decreases with raising values of M. The figure 12 shows the outcome of m on $h(\eta)$ which leads velocity falling with raising values of m.

The result of Casson fluid parameter, unsteady parameter, radiation parameter, Prandtl number, Eckert number, heat absorption/generation parameter on temperature distribution demonstrated in the figures 13-18. Figure 13 display the result of Casson fluid parameter over temperature distribution that represents $\theta(\eta)$ reduced with enhancing cases of β. The effect of unsteady parameter over temperature field $\theta(\eta)$ falling with extending of A which displayed in the figure 14. The outcome of radiation parameter over temperature field indicates $\theta(\eta)$ reduced with raising cases of R which exhibited in the figure 15. Figure 16 illustrates the result of Prandtl number over temperature distribution $\theta(\eta)$ which defines $\theta(\eta)$ falling with raising values of Pr. Figure 17 and Figure 18 displays the effect of Eckert number and heat absorption/generation parameter which describes the temperature field reduced with both increasing cases of Ec and λ.

The figure 19-21 represents the result of concentration profile over unsteady parameter, Schmidth number and chemical reaction parameter. The outcome of unsteady parameter on concentration distribution displayed in figure 19 which shows that $\varphi(\eta)$ reduced with variation of A. Figure 20 and 21 shows the outcome of Schmidth number and chemical reaction parameter over concentration profile which demonstrates $\varphi(\eta)$ falling with various values of Sc and γ.

Conclusion

The study of Casson fluid flow over inclined stretching surface with Hall current and viscous dissipation plays a important role on flow has high viscosity such as oil and polymers.

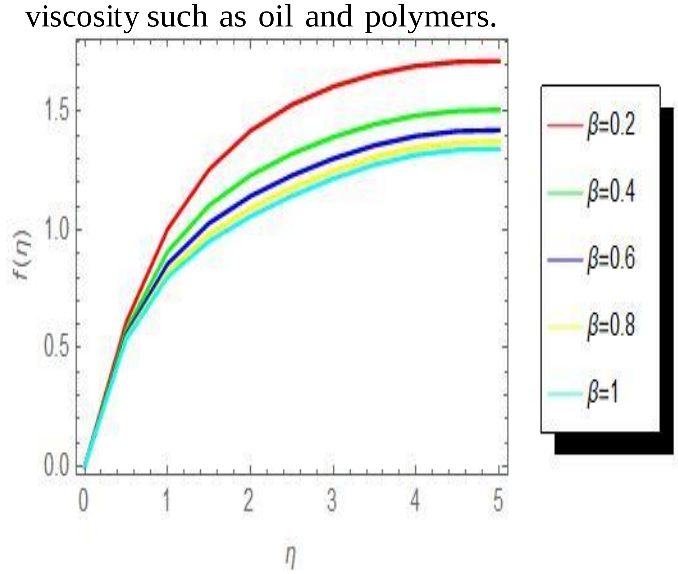

Fig. 2: Outcome of Casson fluid parameter β on velocity field $f(\eta)$.

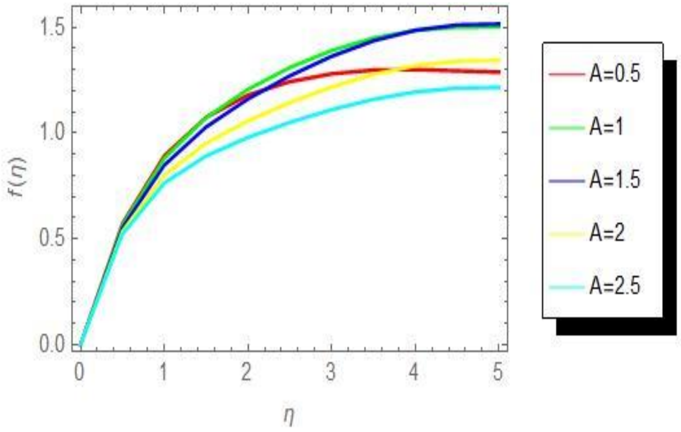

Fig. 3: Outcome of unsteady term A on velocity distribution $f(\eta)$.

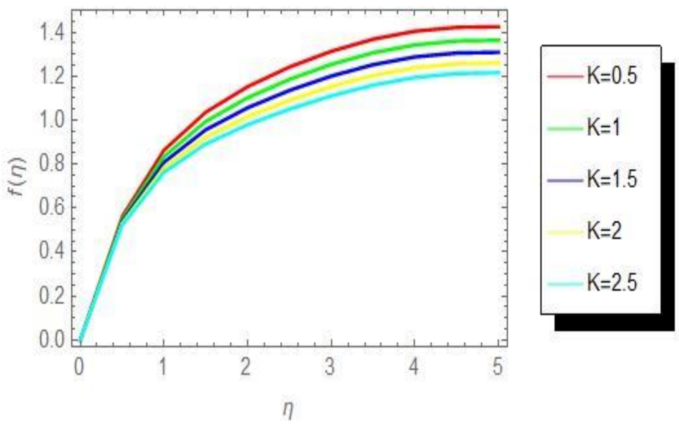

Fig. 4: Result of porosity parameter K over velocity field $f(\eta)$.

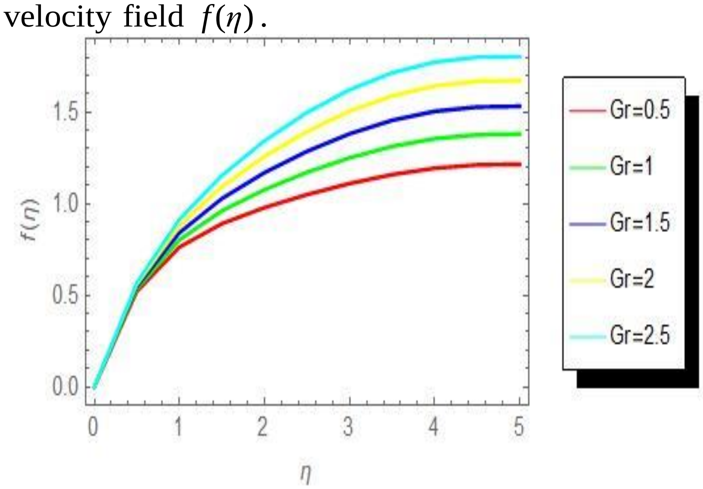

Fig. 5: Outcome of Grashof number Gr on velocity distribution $f(\eta)$

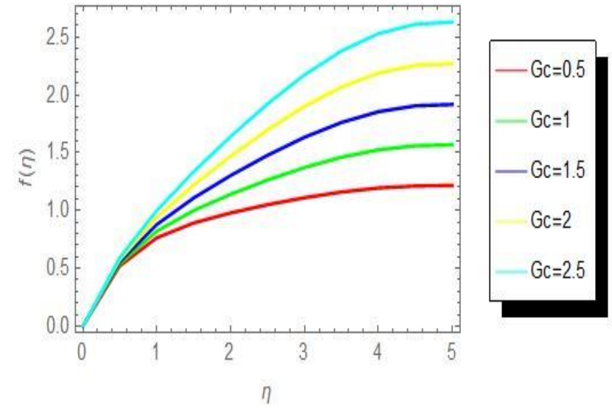

Fig. 6: Impact of modified Grashof number Gc on velocity distribution $f(\eta)$.

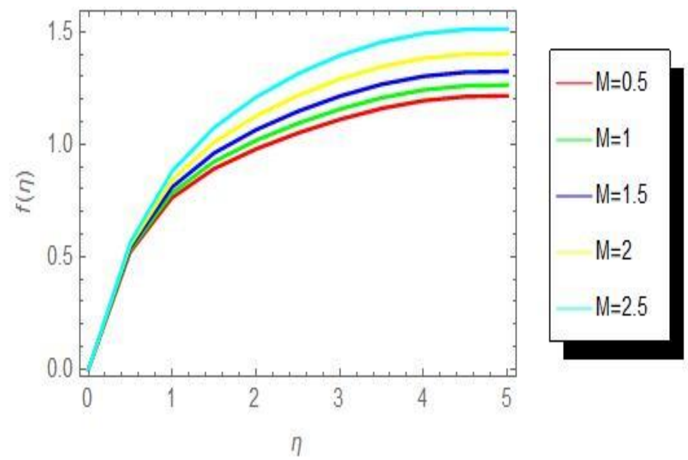

Fig. 7: Result of Magnetic parameter M over velocity distribution$(f(\eta)$.

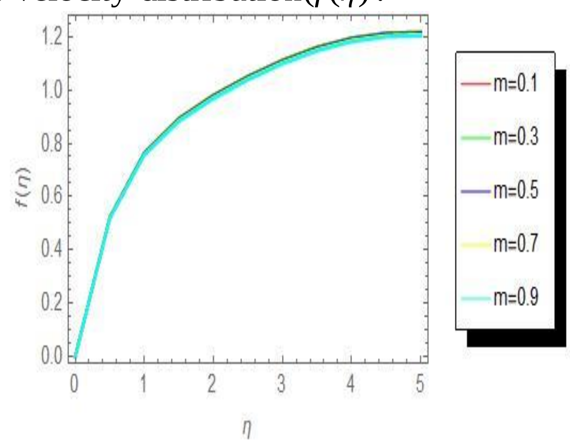

Fig. 8: Influence of Hall current term m over velocity distribution $f(\eta)$.

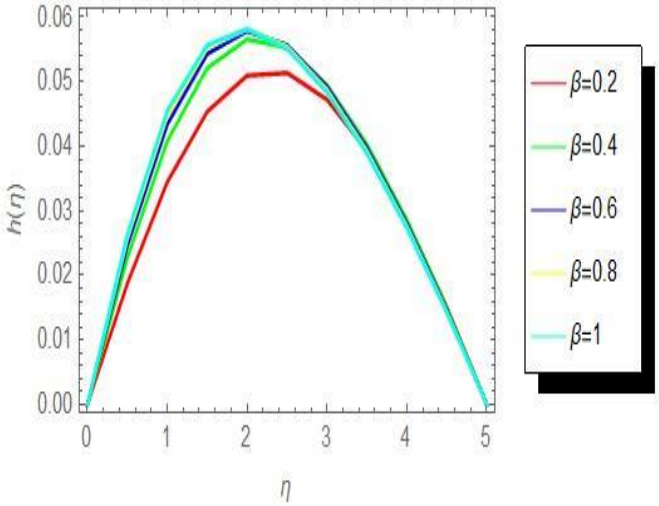

Fig. 9: Variation of Casson fluid parameter β over velocity distribution $h(\eta)$.

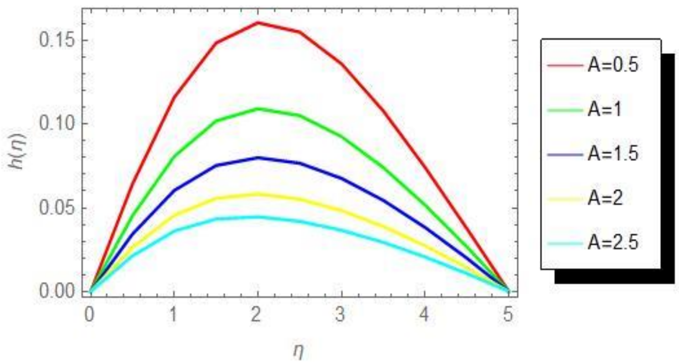

Fig. 10: Result of unsteady parameter A on velocity distribution $h(\eta)$.

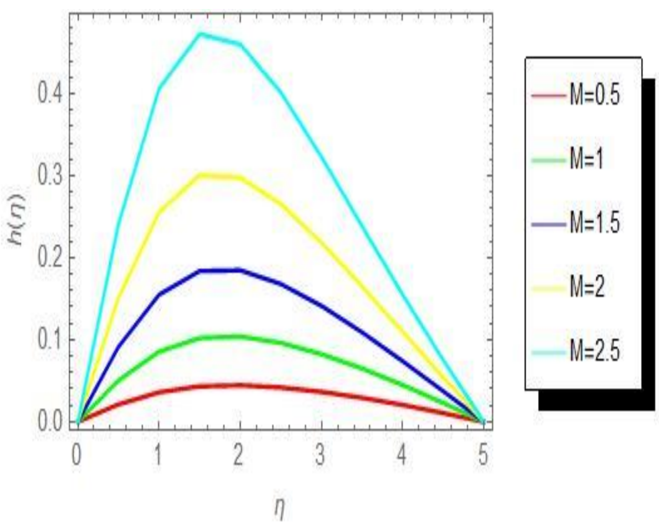

Fig. 11: Outcome of magnetic parameter M on velocity distribution $h(\eta)$.

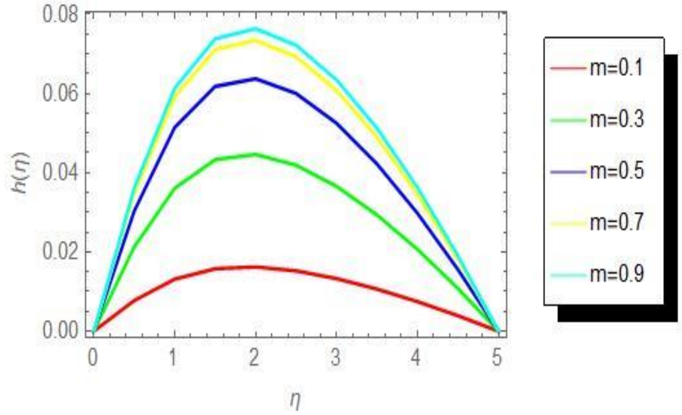

Fig.12: Influence of Hall current term m on velocity distribution $h(\eta)$.

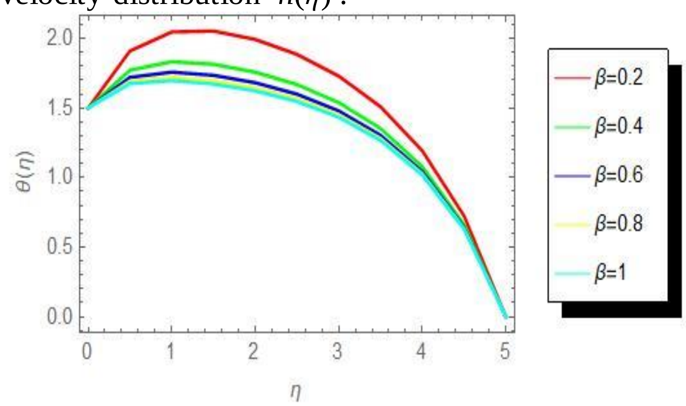

Fig. 13: Outcome of casson fluid parameter β

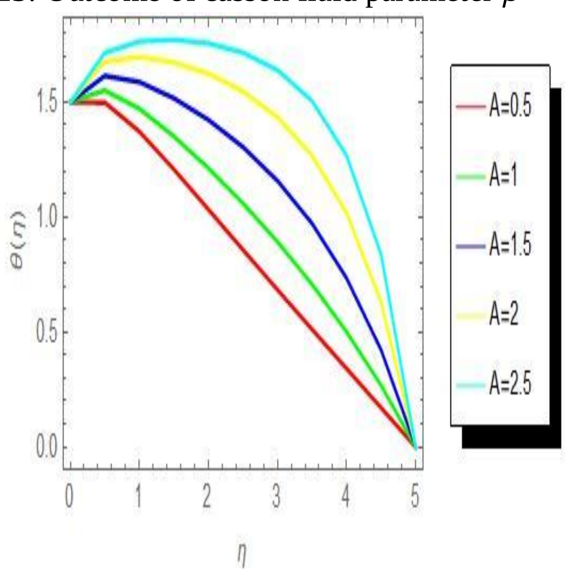

Fig. 14: Consequence of funsteady term A over temperature distribution (η)

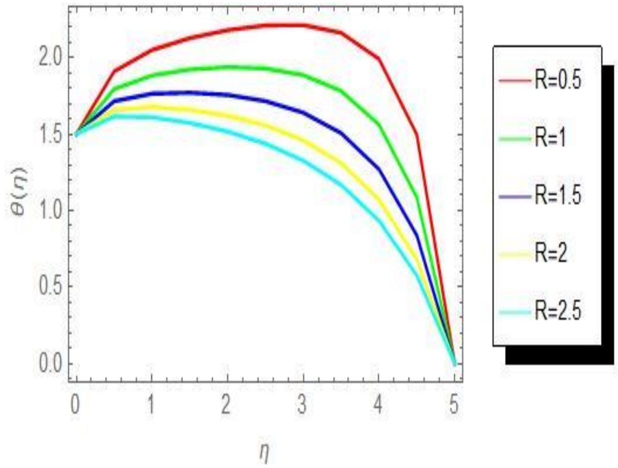

Fig. 15: Influence of radiation parameter R over temperature distribution (η) .

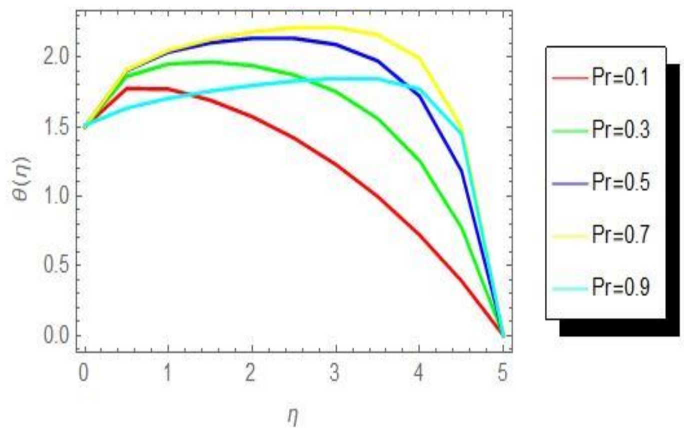

Fig. 16: Influence of Prandtl number Pr on temperature distribution $\theta(\eta)$.

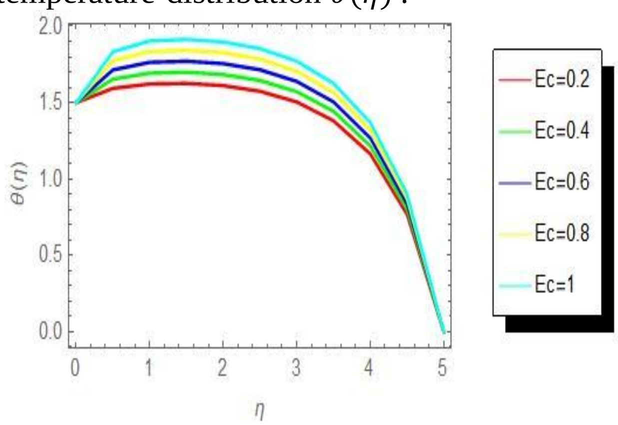

Fig. 17: Outcome of Eckert number Ec over temperature distribution$\theta(\eta)$.

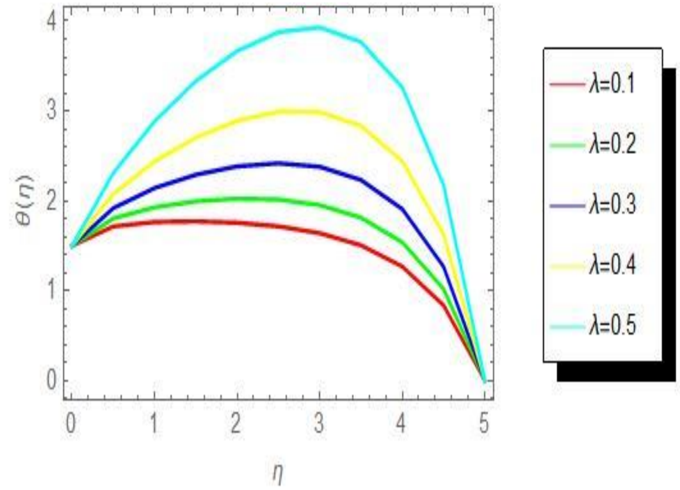

Fig. 18: Result of heat absorption/Generation parameter

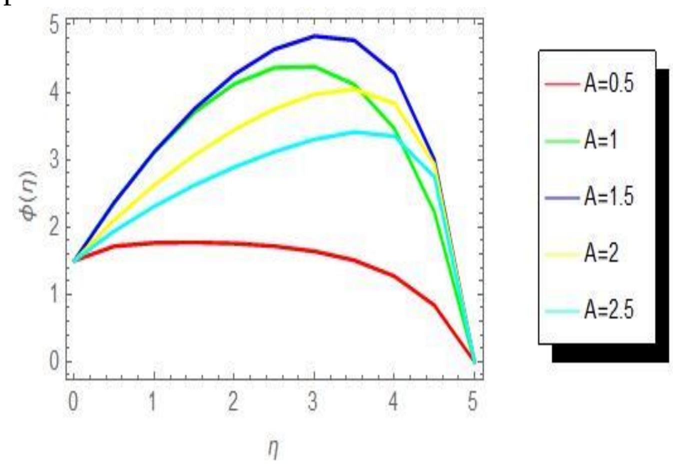

Fig. 19: Variation of unsteady parameter A over concentration (η).

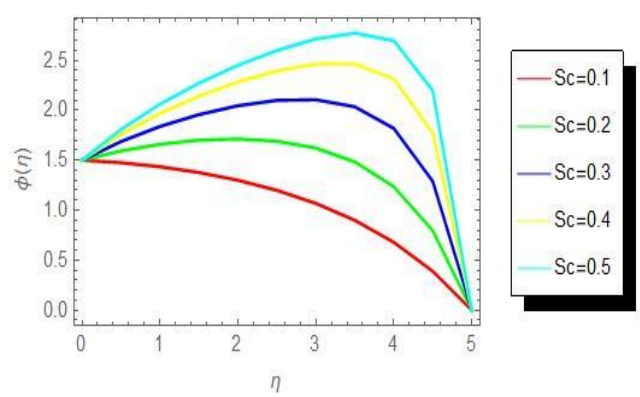

Fig. 20: Outcome of Schmidth number Sc on distribution $\varphi(\eta)$

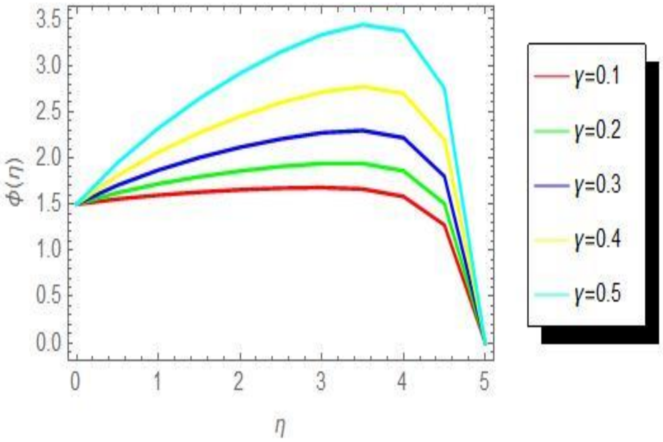

Fig. 21: Impact of chemical reaction term γ on concentration distribution $\varphi(\eta)$

Reference

1. Afridi, M.I., Qasim, M. Khan, I. Sharidan, S and Alshomrani, A.S. (2017), Entropy generation in magnetohydrodynamic mixed convection flow over an inclined stretching sheet, *Entropy*, 19(10), 10.
2. Ali, M., Alam, M. S. Alam, M.,M and Alim, M.,A. (2014), Radiation and thermal radiation effect on a steady MHD free convection heat.
3. Ali, M. and Alam, M.,S. (2014), Soret and Hall effect on MHD flow, heat and mass transfer over a vertical stretching sheet in a porous medium due to heat generation, *ARPN Journal of Engineering and Applied Science*, 9(3), 361-371.
4. Bilal Asharf, M., Hayat, T and Alsaedi, A. (2017), Mixed convection flow of casson fluid over a stretching sheet with convective boundary conditions and Hall effect, *Boundary Value Problems*, 2017(1), 137.
5. Eswara Rao, M. (2017), The effects of thermal radiation and chemical reaction on MHD flow of a Casson fluid over and exponentially inclined stretching surface, *Journal of Physics Conference Series*, 1000(1),2997- 3006.
6. Imran Ullah, Sharidan Shafie and Ilyas Khan. (2017), Effects of slip condition and Newtonian heating on MHD flow of Casson fluid over a non linearly stretching sheet saturated in a porous medium, *Journal of King saud University-Science*, 29(2), 250-259.
7. Mahanta, G and Shaw, S. (2015), 3D Casson fluid flow past a porous linearly stretching sheet with convective boundary condition, *Alexandria Engineering Journal*, 54(3),653-659.
8. Manjula, V and Chandra Sekhar, K.V. (2020), Analysis of Heat and mass transfer on steady MHD Casson fluid flow past an Inclined porous stretching sheet with viscous dissipation and thermal radiation, *International Journal of Mechanical and Production Engineering Research and Development(IJMPERD)*, 10(3),281-292.
9. Mustafa, M., Hayat, T. Pop, I and Aziz, A. (2011), Unsteady boundary layer flow of a Casson fluid due to an impulsively started moving flat plate, *Heat Transfer-Asian Research*, 40(6),536-576.
10. Nadeem, S., Haq, R.U. Akbar, N.S and Khan, Z.H. (2013). MHD three dimensional Casson fluid flow past a porous linearly stretching sheet, *Alexandria Engineering Journal*,52(4),577-582.
11. Pavan Kumar, C., Raghunath, K and Obulesu, M. (2021). Thermal diffusion and inclined magnetic field effects on mhd free convection flow of Casson fluid past an inclined plate in conducting field, *Turkish Journal of Computer and Mathematics Education*, 12(13), 960-977.
12. Raju, C.S.K., Sandeep, N. Sugunamma, V. Jayachandra Babu, M and Ramana Reddy, J.V. (2016). Heat and mass transfer in magnetohydrodynamic Casson fluid over an exponentially permeable stretching surface, *Engineering Science and Technology an International Journal*, 19(1),45-52.
13. Shateyi, S., Mabood, F and Lorenzini, G. (2017). Casson fluid flow: free convective heat and mass transfer over an unsteady permeable stretching surface considering viscous dissipstion, *Journal of Engineering Thermophysics*, 26(1), 39-52.
14. Srinivasa Raju, R., Mahesh Reddy, B and Jithender Reddy, G. (2017),.Finite element

solutions of free convective Casson fluid flow past an vertically inclined plate submitted in Magnetic field in presence of heat and mass transfer, *International Journal for Computational Methods in Engineering Science and Mechanics*, 18(4-5), 250-265.

15. Swati Mukhopadhyay., Prativa Ranjan De. Krishnendu Bhattacharyya and Layek, G.C. (2013). Casson fluid flow over an unsteady stretching surface, *Ain Shams Engineering Journal*,4(4),933-938.
16. Tabaei, H., Moghimi, M.A. Kimiaeifar, A and Moghimi, M.,A. (2011). Homotopy analysis and differential quadrature solution of the problem of free-convective magnetohydrodynamic flow over a stretching sheet with the Hall effect and mass transfer taken into account, *Journal of Applied Mechanics and Technical Physics*, 52(4), 624-636.
17. Turkyilmazoglu, M., (2011), Thermal radiation effects on the time- dependent MHD permeable flow having variable viscosity, *International Journal of Thermal Sciences*, 50(1),88-96.

*****